PHYSICAL REVIEW D VOLUME 35, NUMBER 11 1 JUNE 1987

Transverse momentum in high-energy nuclear collisions: Collective expansion

Xin-nian Wang and Rudolph C. Hwa
Institute of Theoretical Science and Department of Physics, University of Oregon, Eugene, Oregon 97403
(Received 29 December 1986)

Hadron production in the central region in high-energy nuclear collisions is investigated. The hydrodynamical expansion of a locally thermalized system is studied for both the cases with and without phase transition. The case with phase transition is considered by using a sound-velocity function $c_s(T)$ parametrized to fit the energy density determined in a lattice gauge calculation. The effect of a transverse rarefaction wave is included in the calculation of the temperature profile of the expanding fluid. The transverse-momentum distribution of hadrons is calculated by collecting all the hadrons produced when the hadron gas is cooled down to a freeze-out temperature at different times in the expansion. Fluctuation in initial temperature and radius is allowed due to variation in impact parameter. On the basis of a study of the thermalization process in the parton model we impose a constraint on the initial temperature and the thermalization time, the simultaneous variation of both of which gives rise to a relationship between the average transverse momentum and rapidity density. We have found that there is no so-called "plateau" region in that relationship. The implication on the diagnostics of a quark-gluon plasma is discussed.

I. INTRODUCTION

For many years the average transverse momentum $\langle p_T \rangle$ of produced particles in high-energy hadronic collisions has been found to have the characteristic value 350 MeV/c in the minimum-bias events, essentially independent of the incident energy or incident particles. It has been regarded as a feature that is a consequence of the spatial size of the hadrons, but no detailed theory has been advanced to calculate its value, which is the trademark of low-p_T physics.

Recently, it has been established experimentally that $\langle p_T \rangle$ increases with energy in $\bar{p}p$ collisions[1,2] for $\sqrt{s}$ above 200 GeV, and depends on the multiplicity of produced particles in the cosmic-ray Japanese-American Cooperative Emulsion Experiment[3] (JACEE) in such a way that $\langle p_T \rangle$ first increases to a region in which the data points are widely scattered and then rises again at higher rapidity density dN/dy. Indeed, it has been suggested[4] that the plateau could be interpreted as a possible signature for a first-order phase transition into quark-gluon plasma. The dependence of $\langle p_T \rangle$ on dN/dy has more recently been studied[5] in a model for particle production in AA collisions, in which it is assumed that the hot matter formed after collision is a collection of spherically exploding plasma droplets in hydrodynamical expansion. The local spherical symmetry drastically simplifies the calculation so that $\langle p_T \rangle$ can be obtained as a function of temperature T without solving first the hydrodynamical equations. Using certain assumptions to relate the energy density to the observed rapidity density, the agreement between the prediction of the model and the JACEE data is claimed to be good.

The most comprehensive study to date of the transverse-momentum distribution is, as far as we know, the work reported in Ref. 6, in which many issues related to the evolution of matter produced in ultrarelativistic nuclear collisions have been considered. After some detailed hydrodynamical calculations, their results only vaguely suggest the existence of a plateau region in $\langle p_T \rangle$ versus dN/dy, and the sharp rise at higher dN/dy is visible only in the logarithmic scale of dN/dy. In their study they have approximated the energy-density function $\epsilon(T)$ by a step function, and have fixed the initial nuclear radius for each reaction while putting in fluctuation in initial temperature by hand.

In this paper we investigate the hydrodynamical-flow problem in a way similar in spirit to that in Ref. 6, but impose different conditions both at the start of the transverse expansion and at freeze-out. We also treat phase transition differently. In outline we study in detail a cylindrically expanding hydrodynamical system and consider both the case of having a phase transition and without such a transition. Due attention will be paid to the collective effect of the transverse rarefaction wave. The transverse momentum of the hadrons is calculated by studying the temperature profile of the system as a function of time and by assuming that the expanding hadron gas freezes out at a temperature T_f, whose value can be restricted to a very narrow range. Phase transition is introduced into the calculation by parametrizing the sound velocity c_s as a function of T in accordance to the result determined in a lattice gauge calculation.[7] Fluctuation in the initial temperature T_0 is assumed to be related to the variation in impact parameters among the collisions so that the initial radius and T_0 are coupled. In this respect our work differs significantly from that in Ref. 6. We allow T_0 and τ_0, the thermalization time, to vary subject to a constraint derived in thermalization study in the parton model.[8] Thus even for an experiment with fixed beam and target nuclei at fixed incident energy, the effective nucleon number A varies with impact parameter, resulting in simultaneous variation in T_0 and τ_0. Apart from this difference our approach to the problem is very similar to

that of Ref. 6. We do not consider the possibility of shock waves, a treatment of which has been considered in Ref. 9.

The thermodynamical and hydrodynamical aspects of our problem are intrinsically coupled together in the theory so that in our calculation of the p_T distribution of the produced hadrons it is not possible to separate $\langle p_T \rangle$ into two distinct corresponding components. Thus our result has a definite bearing on the suggestions made in Refs. 4 and 5 that $\langle p_T \rangle$ exhibits a plateau as a function of increasing dN/dy before rising again, a phenomenon purported to be related to the deconfinement transition in high-energy nuclear collision. Indeed, our conclusion is that the curve for $\langle p_T \rangle$ versus dN/dy does not behave that way.

In a paper to follow, the contribution to $\langle p_T \rangle$ arising from minijets produced by the hard scattering of partons will be described. Since minijets originated from a quark-gluon plasma will depend on the characteristics of the transverse hydrodynamical expansion, the subject of concern in this paper carries a significance that goes beyond the results to be presented below.

II. HYDRODYNAMICAL EXPANSION

For simplicity we consider first a head-on collision between two identical nuclei at very high energy so that initially we have a disk of strongly interacting system whose constituents are either quarks and gluons or hadrons depending on whether there is or is not deconfinement, respectively. To avoid stating the two cases in parallel repeatedly, we shall in the following focus on the case where the initial temperature T_0 is high enough and the thermalization time τ_0 is short enough so that deconfinement does occur. The case of no phase transition can be treated easily as a special case and will not be mentioned until the results are to be presented near the end.

We assume that the system of quarks and gluons quickly achieves local thermal equilibrium in a time scale τ (proper time) less than 1 fm/c. Persuasive arguments can be given to justify this assumption by analyzing the thermalization process on the basis of some reasonable estimates,[6] or in the framework of the parton model.[8] While the initial values T_0 and τ_0 are relevant for the numerical calculations later, our description of the time evolution of the system here relies only on the property that the system reaches local thermal equilibrium before it enters the process of hydrodynamical expansion. We adopt the scaling description of that expansion advanced by Bjorken.[10] Thus the space-time picture of the system is that the hot matter has a cylindrical symmetry, the two leading edges of the cylinder receding at rapidities comparable to those of the incident nuclei. In the central region which is the region of interest to us here, there is Lorentz invariance under longitudinal boost. In any frame the longitudinal flow velocity v_z depends on space (z) and time (t) in the simple scaling manner $v_z = z/t$. In the transverse plane at any z in the central region the fluid expands symmetrically in the radial direction, thus setting up a rarefaction wave that propagates inward. The hydrodynamical description of the transverse flow is given in detail by Baym *et al.* (BFBSC),[11] whose work we shall follow closely. We give here a brief summary of the key points that are relevant to our calculation.

Assuming no dissipation or creation of matter, the stress-energy tensor $T^{\mu\nu}$ satisfies the continuity equation

$$\partial_\mu T^{\mu\nu} = 0 , \tag{2.1}$$

where in the metric $g^{00}=1$, $g^{ii}=-1$, $T^{\mu\nu}$ can be written as

$$T^{\mu\nu} = (\epsilon + P) u^\mu u^\nu - P g^{\mu\nu} . \tag{2.2}$$

Here ϵ is the energy density, P the pressure in the comoving frame, and u^μ is the fluid velocity vector. The sound velocity is given by

$$c_s^2 = \frac{\partial P}{\partial \epsilon} = \frac{\partial}{\partial} \frac{\ln T}{\ln s} , \tag{2.3}$$

where s is the entropy density, the conservation of which,

$$\partial_\mu (s u^\mu) = 0 , \tag{2.4}$$

follows from (2.1), (2.2), and $\epsilon + P = Ts$, the enthalpy density. For the one-dimensional problem of longitudinal expansion, Bjorken's scaling solution has the property

$$s(\tau) \propto \tau^{-1} , \tag{2.5}$$

where τ is the proper time

$$\tau = (t^2 - z^2)^{1/2} . \tag{2.6}$$

For the transverse expansion that is concurrent with the longitudinal expansion, we need only consider, by virtue of the longitudinal-boost invariance, the transverse plane at $z=0$, in which the radial coordinate r and velocity v_r are the only essential variables. In terms of the transverse rapidity variable

$$\alpha = \operatorname{arctanh} v_r \tag{2.7}$$

it can be shown from (2.1) and (2.4) that the transverse hydrodynamical equations on s and T can be expressed in the form[11]

$$\frac{\partial}{\partial \tau}(r \tau s \cosh\alpha) + \frac{\partial}{\partial r}(r \tau s \sinh\alpha) = 0 , \tag{2.8a}$$

$$\frac{\partial}{\partial \tau}(T \sinh\alpha) + \frac{\partial}{\partial r}(T \cosh\alpha) = 0 . \tag{2.8b}$$

Introducing the function $\Phi(T)$, defined by

$$d\Phi = c_s^{-1} d \ln T = c_s d \ln s \tag{2.9}$$

where c_s need not be a constant, BFBSC recast (2.8) in terms of the functions

$$a_\pm(r,\tau) = \exp(\Phi \pm \alpha) \tag{2.10}$$

which then satisfy the characteristic equations

$$(1 \pm v_r c_s) \frac{\partial a_\pm}{\partial \tau} + (v_r \pm c_s) \frac{\partial a_\pm}{\partial r} + c_s \left[\frac{v_r}{r} + \frac{1}{\tau} \right] a_\pm = 0 . \tag{2.11}$$

These equations have been solved[11] numerically as well as analytically (in a certain approximation close to the

Riemann solution), both for constant c_s. From the solution for $a_\pm$, the value of Φ can be obtained by inverting (2.10), i.e.,

$$\Phi=\tfrac{1}{2}\ln a_+ a_- , \tag{2.12}$$

whereupon (2.9) yields

$$T=T_0 e^{c_s\Phi} . \tag{2.13}$$

The value of v_r can be determined more directly by use of

$$v_r=\frac{a_+-a_-}{a_++a_-} . \tag{2.14}$$

For our problem where c_s is not constant due to phase transition, we cannot use the analytic method of solving (2.11), so the numerical procedure is our only recourse, once the T dependence of c_s is specified. In place of (2.13), an inversion of

$$\Phi(T)=\int_{T_0}^{T}[T'c_s(T')]^{-1}dT' \tag{2.15}$$

becomes necessary, after the integration is performed.

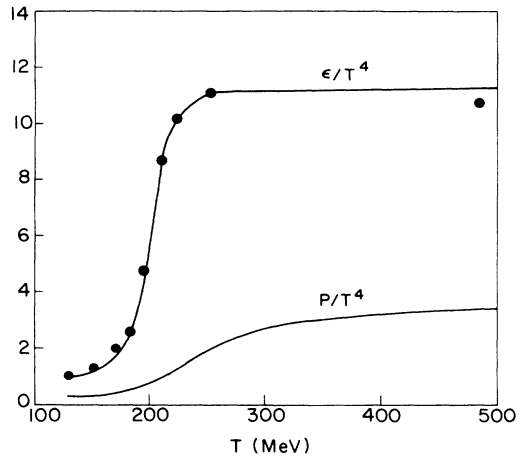

FIG. 1. Plots of ϵ/T^4 and P/T^4 vs T. The points are the results of the lattice gauge calculation obtained in Ref. 7. The curve for ϵ/T^4 is a plot of Eq. (3.6) in the text. P/T^4 is calculated from that parametrization. The critical temperature T_c is set at 200 MeV.

III. SOUND VELOCITY WITH PHASE TRANSITION

For the purpose of our calculation in the following we want to have an analytic form for the sound velocity, $c_s(T)$, that contains the effects of a phase transition. From the thermodynamical relation

$$\epsilon=T^2\frac{\partial}{\partial T}(P/T) , \tag{3.1}$$

we can relate the dimensionless quantities $\hat{\epsilon}(T)$ and $\hat{p}(T)$, defined by

$$\epsilon(T)=T^4\hat{\epsilon}(T) \tag{3.2}$$

and

$$P(T)=T^4\hat{p}(T) \tag{3.3}$$

by the integral

$$\hat{p}(T)=T^{-3}\int_0^T\hat{\epsilon}(T')T'^2dT' . \tag{3.4}$$

Then, from (2.3) we obtain

$$c_s^2(T)=\frac{\hat{\epsilon}(T)+\hat{p}(T)}{4\hat{\epsilon}(T)+Td\hat{\epsilon}(T)/dT} . \tag{3.5}$$

Hence, knowledge of $\hat{\epsilon}(T)$ will enable us to calculate $c_s(T)$.

For $\hat{\epsilon}(T)$ we turn to the result of lattice calculation in QCD. Celik, Engels, and Satz[7] have performed a Monte Carlo calculation on an $8^3\times 3$ lattice with dynamical quarks ($N_f=2$) in SU(3) gauge theory, and obtained $\hat{\epsilon}(T)$ as shown in Fig. 1. The deconfinement transition results in a rapid but apparently smooth change at around a critical temperature $T_c\cong 155\Lambda_L$ where Λ_L is the (arbitrary) lattice scale. The boundedness of $d\hat{\epsilon}(T)/dT$ at T_c implies, according to (3.5), that the second velocity c_s does not vanish there. This does not necessarily imply the absence of a first-order phase transition, for which $P(\epsilon)$ is a constant in the transition region, and consequently $c_s=0$ as required by (2.3). The nonvanishing of c_s could well be due to the finite-volume effects in the lattice calculation.

For our purpose below which is to take into account the effects of phase transition on the p_T distribution of produced hadrons, we need not be involved in any speculation on the detailed nature of the phase transition. It is sufficient for us to make use of $\hat{\epsilon}(T)$, given in Fig. 1, as input to our calculation. We therefore parametrize $\hat{\epsilon}(T)$ as

$$\hat{\epsilon}(T)=B+(A-B)[1+\exp(T_c-T)/b]^{-1} . \tag{3.6}$$

Choosing the values $A=11.34$, $B=0.99$, and $b=0.0516T_c$, we obtain the result shown by the solid curve in Fig. 1. There is no physical significance in the specific choice of the form in (3.6), apart from its common usage to describe a rounded step function. We are not seriously concerned with the discrepancy between the curve and the points from lattice calculation in Fig. 1 for $T<T_c$ because in that region the quarks and gluons condense into hadrons; thus the behavior of $\hat{\epsilon}(T)$ there depends on the details of the hadronization process, which in turn is sensitive to the lattice size chosen. Since in both the lattice calculation and our calculation of the hadron momentum in the next section the hadronization process is treated in some degree of approximation, we feel that our simple parametrization of $\hat{\epsilon}(T)$ in (3.6) is totally adequate for our purpose.

Since the temperature in (3.6) is measured in units of Λ_L^{-1}, which is arbitrary, we shall, in applying (3.6), assume a typical value for T_c, such as 200 MeV. The result will not critically depend on the precise value of T_c.

Using (3.6) in (3.4) and (3.5), we have calculated $c_s^2(T)$, which is shown in Fig. 2. Evidently, $c_s^2(T)$ has a deep dip at $T\cong T_c$. On the two wings, c_s^2 has the ideal-gas value of $\frac{1}{3}$. The width of the dip is characterized by the value of b in (3.6), which is chosen to fit the points in Fig.

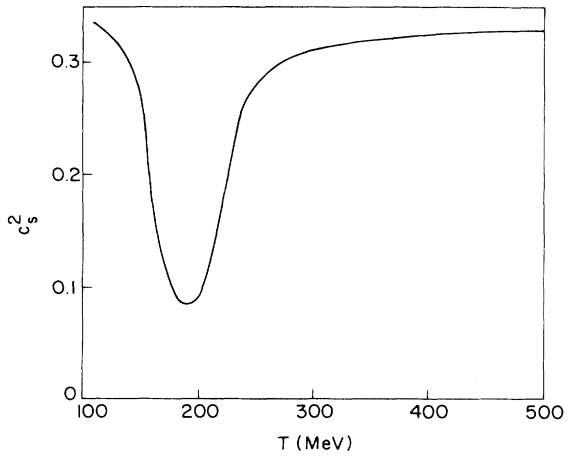

FIG. 2. Sound velocity squared $c_s^2(T)$.

1 for $T \geq T_c$. If one uses the points for $T < T_c$ to determine directly the value of $c_s^2(T)$ in that region, one would find that[12] $c_s^2(T) < \frac{1}{3}$ where our result has already reached the ideal-gas value. We note that the behavior of our $c_s^2(T)$, in particular its value at $T \cong 140$ MeV being $\frac{1}{3}$, is consistent with our later treatment of the pion gas at freeze-out when the pions are regarded as noninteracting massless particles. Conversely, without using the parametrization (3.6), the sound velocity inferred[12] directly from current lattice calculations would have implied a hadron gas whose dynamics is so complicated at freeze-out that there would be no consistent method to treat the transverse-momentum distribution quantitatively.

In summary, on the basis of (3.5) and (3.6) we shall regard in the following the velocity of sound $c_s(T)$ as known numerically.

IV. NUMERICAL SOLUTION FOR TRANSVERSE EXPANSION

We now combine the results of Secs. II and III to solve for the transverse expansion. Let τ_0 denote the time when the transverse expansion beings, R the initial radius, and T_0 the initial temperature of the locally thermalized fluid. The initial conditions are

$$T(r,\tau_0)/T_0 = \Theta(R-r) , \tag{4.1}$$

$$v_r(r,\tau_0) = \Theta(r-R) . \tag{4.2}$$

The second equation above is equivalent to no radial fluid velocity at all $r > 0$, since no fluid exists initially for $r > R$. However, for $\tau > \tau_0$, the solution approaches (4.2) in the limit $\tau \rightarrow \tau_0$.

The numerical integration of (2.11) is performed by the method of characteristics.[11,13] Because $c_s^2(T)$ is a smoothly varying function of T, we have no difficulty in executing the integration of the characteristic equations by finite differences, contrary to what one might encounter if $c_s^2(T)$ were sharply discontinuous, as would be the case in the bag-model description of phase transition. For definiteness, we have taken $\tau_0 = 1$ fm/c and $R = 7$ fm in this part of our calculation.

The results of our calculation are shown in Figs. 3–6. We show in Fig. 3 T/T_0 as a function of r for various values of τ. The two sets of curves correspond to the two cases: $c_s^2 = \frac{1}{3}$ (no transition, dashed curves) and $T_c/T_0 = 0.5$ (with transition, solid curves). The same are shown in Fig. 4, except that $T_c/T_0 = 0.3$ for the solid curves. It is clear in each case that there is a radial rarefaction wave propagating inward from $r = R$, while the fluid expands rapidly outward radially (as well as longitudinally, though not evident from the figure). It is also clear from the figures that in the cases with phase transition, as the interior temperature reaches T_c, the fluid stays at that temperature for a long time. During this long period when the system is in the mixed phase, the fluid continues to expand, thereby lowering its energy density, as the latent heat is converted into kinetic energy. As is evident from Figs. 3 and 4, the solid curves are always higher than the dashed curves of the same τ. It therefore implies that the radius of the part of the fluid that has cooled down to a given temperature is always greater for the case with phase transition than that for the case without. This feature of the hydrodynamical expansion will be important immediately below in determining the transverse velocity of the fluid in the two cases.

In solving the hydrodynamical equation (2.11) the transverse velocity v_r is simultaneously obtained along with the determination of $T(r,\tau)$. The results for $v_r(r,\tau)$ are shown in Figs. 5 and 6, again for the same two values

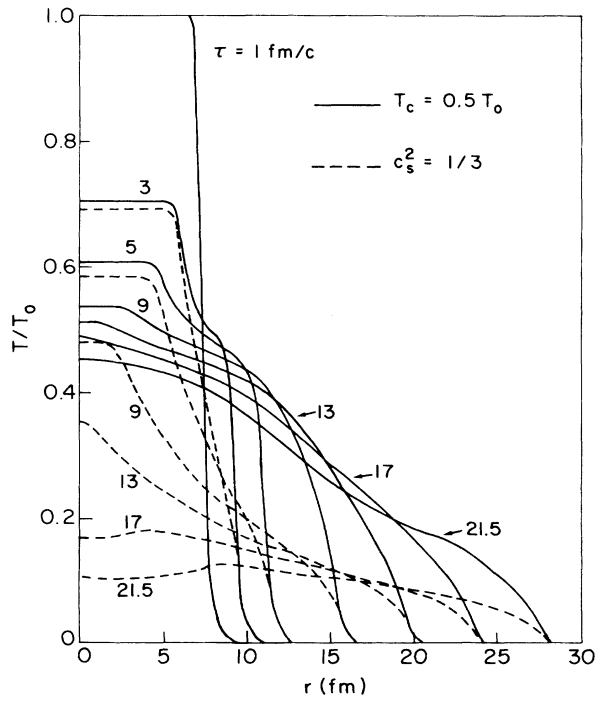

FIG. 3. Temperature profile at various values of τ. Solid line is for the case with phase transition of ($T_c = 0.5T_0$), the dashed line without. For these curves, we have set $R = 7$ fm and $\tau_0 = 1$ fm/c.

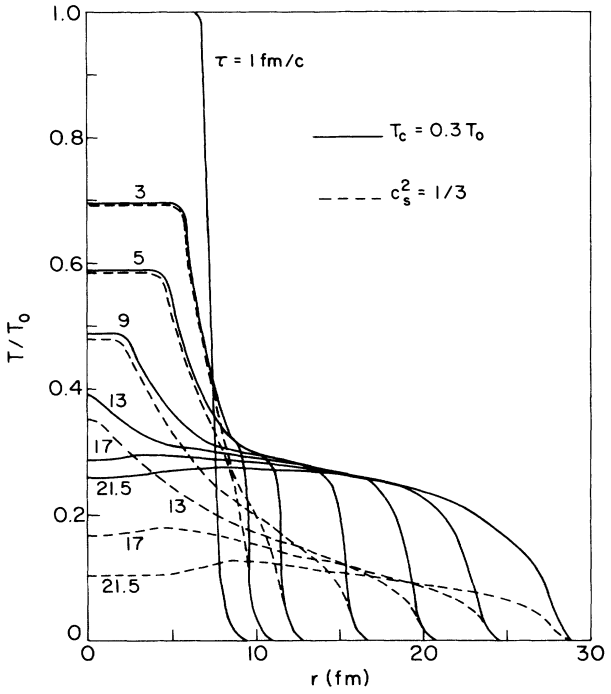

FIG. 4. Same as for Fig. 3, except that $T_c/T_0=0.3$.

of T_c. It is a general property in these solutions that at any given τ the velocity increases monotonically with r, while roughly speaking, v_r decreases (increases) with τ at a fixed $r > R$ ($< R$). We also see in these figures that the curves for having phase transition (solid) are always lower than the ones without (dashed) for the same values of τ. This, however, does not mean that the fluid velocity for the former is lower. It is important to compare the values of v_r for the two cases *at the same temperature.* For a calculation of p_T of the produced hadrons, the relevant temperature is the one when the hadron gas freezes out. At $T=T_f$, the freeze-out temperature, the hadrons undergo free streaming without further interaction. If we now apply the conclusion of the preceding paragraph to the present consideration at T_f, which must be less than T_c, we see that the value of $v_r(r,\tau)$ for the case with phase transition at a given τ and at the value of r corresponding

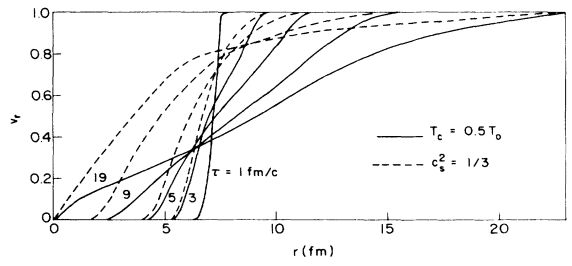

FIG. 5. Transverse velocity in unit of c at various values of τ. Other parameters are as in Fig. 3.

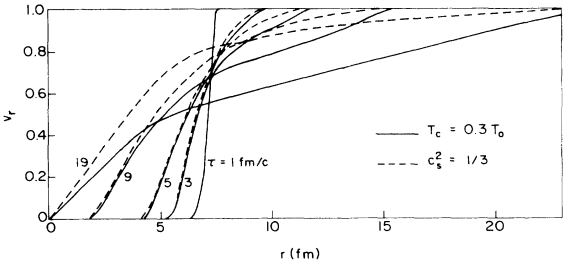

FIG. 6. Same as for Fig. 5, except that $T_c/T_0=0.3$.

to some T_f (using Fig. 3 or 4) is always *higher* than that without phase transition at the same τ and T_f (consequently, at smaller r). For this reason a phase transition leads to higher transverse velocities and therefore higher transverse momenta of the produced hadrons, which we shall quantify in the next section.

In Figs. 7 and 8 we show the transverse velocities $v_r(\tau)$ as functions of τ at various values of T for $T_c/T_0=0.5$ and 0.3, respectively. In each of those figures we again exhibit the two sets of curves with (solid) and without (dashed) phase transition for comparison. Note that when T is significantly greater than T_c, the values of $v_r(\tau)$ for the two cases are very close, obviously because the effect of phase transition has not yet been experienced by the fluid. After T drops near T_c, differences between the two cases begin to develop: the case with phase transition has higher $v_r(\tau)$ at all τ, as has been mentioned above. A comparison between the solid curves of Figs. 7 and 8

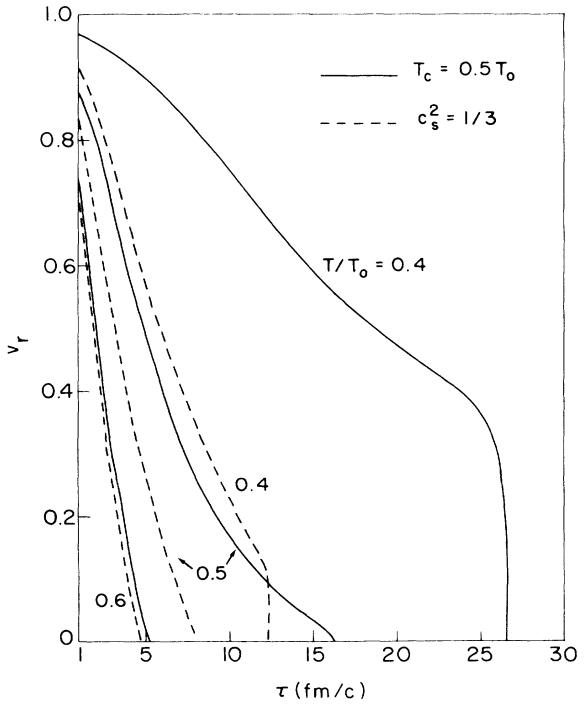

FIG. 7. Transverse velocity as a function of τ for fixed T/T_0. Other parameters are as in Fig. 3.

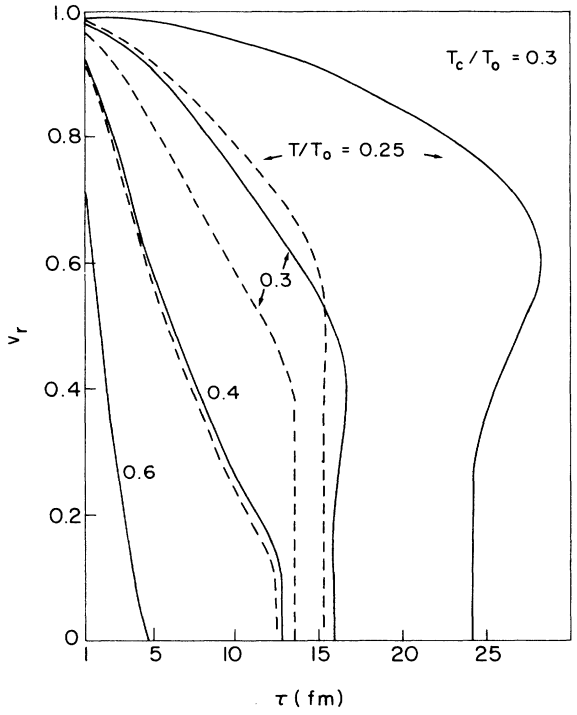

FIG. 8. Same as Fig. 7, except that $T_c T_0 = 0.3$.

would be especially meaningful, if we consider the same values of T_c, T_f, and τ but different T_0 in the two figures. Thus, regard T_0 in Fig. 8 as representing an increase over that in Fig. 7 by a factor of $\frac{5}{3}$. Then for the case T_f in the two cases, T_f/T_0 is decreased by the same factor. Comparing the curve for $T_f/T_0=0.4$ in Fig. 7 with the one for $T_f/T_0=0.25$ in Fig. 8, we see that $v_r(\tau)$ is significantly increased. Hence, we have here a graphic illustration of the dependence of the transverse velocity on the initial temperature: the higher T_0, the more time the system has to expand until freeze-out, and the greater the transverse velocity.

Since different parts of the hadronic fluid take different lengths of time to reach the freeze-out temperature, $v_r(\tau)$ varies over a wide range of τ. A calculation of the average transverse momentum of the produced hadrons must take this phenomenon into account by an integration over τ.

In Fig. 8 one can see that the solid curves at high τ have "partners" with lower v_r that join the ones with higher v_r. These are due to the rarefaction waves being reflected from the origin. In those cases the temperature profile of the system shows a bump in r, as is vaguely evident in Fig. 4 for $\tau=17$ and 21.5 fm/c. The solution of $T(r,\tau)=T_f$ at those values of τ is then double valued. This result in two branches for $\tau>\tau_1$, where τ_1 is defined by

$$T(0,\tau_1)=T_f \tag{4.3}$$

as illustrated in more detail in Fig. 9(b). The two branches meet at τ_f, at which time all hadrons have frozen out.

V. TRANSVERSE-MOMENTUM DISTRIBUTION

There are two stages in the determination of the transverse-momentum distribution of the produced hadrons. The first is the calculation of transverse momentum p_T of a space-time cell which freezes out at T_f when the cell has a transverse velocity v_r. This part of the problem involves statistical averaging. The second stage is to take into account the transverse expansion of the hadron gas when freeze-out can take place over a period of time. This part involves the hydrodynamical characteristics of the whole system which depends on the presence or absence of a phase transition.

We shall consider only pions at freeze-out. Their flux current vector is therefore the statistical average of the pion momentum, averaged over the Bose-Einstein distribution of the pion gas at temperature T, i.e.,

$$J^\mu = \mathcal{N} u^\mu = \frac{g_\pi}{(2\pi)^3}\int \frac{d^3k}{k^0} k^\mu [\exp(k^\mu u_\mu/T)-1]^{-1} , \tag{5.1}$$

where g_π is the degeneracy factor, which is 3 here. It is easier to evaluate the integral in the comoving frame in which $u^\mu=\gamma(1,\mathbf{v}_r,0)$ becomes $u'^\mu=(1,\mathbf{0})$. As in previous sections, we need only consider the $z=0$ plane, so the Lorentz transformation here refers only to the transverse boost by rapidity α, where α is given by (2.7). In terms of the momentum k'^μ in the comoving frame, we have

$$k_0 = k'_0\cosh\alpha + k'_T\sinh\alpha\cos\theta , \tag{5.2a}$$

$$\mathbf{k}_T = \mathbf{k}'_T + \mathbf{v}_r[\mathbf{v}_r\cdot\mathbf{k}'_T(\gamma-1)/v_r^2 + \gamma k'_0] , \tag{5.2b}$$

where $\gamma=(1-v_r^2)^{-1/2}$ and $\cos\theta=\mathbf{v}_r\cdot\mathbf{k}'_T/v_r k'_T$. It then follows from (5.1) and (5.2) that the number density $\mathcal{N}$ is

$$\mathcal{N} = \frac{g_\pi}{(2\pi)^3}\int d^3k'(e^{k'_0/T}-1)^{-1}$$
$$= \frac{g_\pi T^3}{2\pi^2}\sum_{n=1}^{\infty}\frac{\beta^2}{n}K_2(n\beta) , \tag{5.3}$$

where $\beta=m/T$, m being the pion mass, and K_2 is the modified Bessel function.

The transverse momentum p_T of the hadron gas at temperature T is defined by

$$J^0 p_T{}^2 = \frac{g_\pi}{(2\pi)^3}\int \frac{d^{3k}}{k^0} k^0 k_T{}^2 [\exp(k^\mu u_\mu/T)-1]^{-1} . \tag{5.4}$$

Using (5.2) and (5.3), we get

$$p_T{}^2 = T^2\left[\sum_{n=1}^{\infty}\frac{\beta^2}{n}K_2(n\beta)\right]^{-1}$$
$$\times\left[2\sum_{n=1}^{\infty}\frac{\beta^3}{n^2}K_3(n\beta) + \sinh^2\alpha\sum_{n=1}^{\infty}\left[\frac{\beta^4}{n}K_4(n\beta)-\frac{\beta^3}{n^2}K_3(n\beta)\right]\right] . \tag{5.5}$$

We note that in the zero-temperature limit, one obtains the trivial result

$$p_T{}^2 \to (m \sinh\alpha)^2, \quad T \to 0 \ . \tag{5.6}$$

On the other hand, if $\alpha = 0$, we have the thermal transverse momentum

$$p_{T,\mathrm{th}}{}^2 = 2mT \sum_{n=1}^{\infty} n^{-2} K_3(n\beta) \Big/ \sum_{n=1}^{\infty} n^{-1} K_2(n\beta) \ . \tag{5.7}$$

In general, the system is in neither of these unrealistic limits. Instead, we consider the simplification that the pion mass is vanishingly small, an approximation which is not unreasonable for a first-order calculation. Thus, in the limit $m \to 0$, we have

$$\mathcal{N} = \frac{3}{\pi^2} \zeta(3) T^3 \ , \tag{5.8}$$

$$p_T{}^2 = 8 \frac{\zeta(5)}{\zeta(3)} (1 + \tfrac{5}{2} \sinh^2\alpha) T^2 \ , \tag{5.9}$$

where $\zeta(n)$ is the Riemann ζ function. Note that p_T depends on both the temperature and the transverse rapidity, which in turn depend on the nature of hydrodynamical expansion. Evidently, the results described in the preceding section are now needed to proceed further into the second stage of this calculation.

The number of particles (partons and/or hadrons) in the system in the toroidal volume element $dV = 2\pi r \, dr \, dz$ is $J^0 dV$. Since at $z = 0$, $dz = \tau \, d\eta$, where the spatial rapidity η is the same as the velocity rapidity y in the scaling solution, the total number of particles per unit y at $z = 0$ in the fluid within a radius r is

$$\frac{dn(r)}{dy} = 2\pi \int_0^r J^0 r \tau \, dr \ . \tag{5.10}$$

We now consider the freeze-out of hadrons at the outer edge of the cylinder. When the temperature of the surface decreases to T_f at the radius r_f, which is the solution of

$$T(r_f, \tau) = T_f \ , \tag{5.11}$$

the pions leave the hadron gas that is just inside r_f without further interaction. The rapidity density of the pions produced per unit time is then the negative time derivative of (5.10) at freeze-out, i.e.,

$$\frac{d^2N}{d\tau \, dy} = 2\pi J^0 r_f \tau \left[v_r - \frac{\partial r_f}{\partial \tau} \right] \ , \tag{5.12}$$

where use has been made of (2.7) and (2.8a), with $s \cosh\alpha$ being proportional to J^0. In (5.12) J^0 is evaluated at T_f and v_r at $r_f(\tau)$; J^0 is therefore $\mathcal{N} \cosh\alpha$, where $\mathcal{N}$ is the hadron gas density (containing no more unconfined quarks or gluons since $T_f < T_c$). The detected dN/dy, which includes pions produced at all τ, is, therefore,

$$\frac{dN}{dy} = 2\pi \int_{\tau_0}^{\tau_f} J^0 r_f \tau \left[v_r - \frac{\partial r_f}{\partial \tau} \right] d\tau + \frac{dN_{1,2}}{dy} \ . \tag{5.13}$$

The first term on the right-hand side represents the contribution coming from the surface of the hadron gas as the pions there leave the cylindrical system in free streaming. The second term in (5.13) represents the residual contribution, and has two specific forms depending on the hydrodynamical condition at freeze-out.

There are two possible scenarios. First, before the rarefaction wave reaches the origin, the central core region that has zero v_r has already cooled down to T_f due to longitudinal expansion. Then the freezing out of the pions in that region at that time, τ_f, contributes to

$$\frac{dN_1}{dy} = \pi R_f{}^2 \tau_f \mathcal{N}(T_f) \ , \tag{5.14}$$

a result that follows directly from (5.10) and the definition

$$R_f = r_f(\tau_f) \ . \tag{5.15}$$

In Fig. 9(a) we have plotted the temperature profile of the hadronic system in this scenario for the case of no phase transition.

The other possibility is that the rarefaction wave reaches the origin and is reflected before the temperature of the central part of the system reaches T_f. As we have mentioned before at the end of the preceding section, there is then a bump in the temperature profile. This is shown in Fig. 9(b), again for the case of no phase transition, since the effect is most pronounced in that case when T_0 is sufficiently high. At τ_1 freeze-out begins from the central core of the cylinder while an annular ring of the system remains in the gaseous state. This is the second branch for $\tau > \tau_1$. The pions produced in this second branch are represented by the second term in (5.13), which should clearly be

$$\frac{dN_2}{dy} = 2\pi \int_{\tau_1}^{\tau_f} J^0 r_f' \tau \left[\frac{\partial r_f'}{\partial \tau} - v_r' \right] d\tau \ , \tag{5.16}$$

where the integrand is to be evaluated along the second branch, in which the radius and transverse velocity at freeze-out are denoted by r_f' and v_r', respectively [see Fig. 9(b)].

Having indicated the way to compute dN/dy, it is now straightforward to calculate $\langle p_T{}^n \rangle$. To simplify notation, let us define

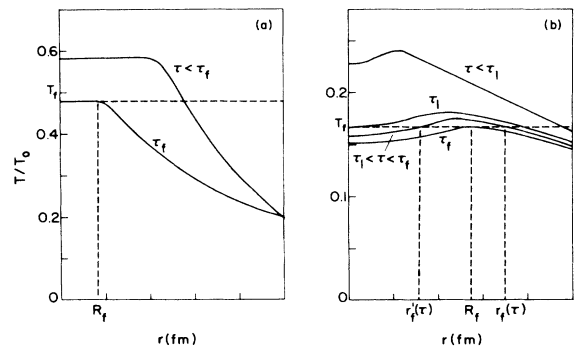

FIG. 9. Temperature profiles at various τ for the case of no phase transition. (a) $T_f/T_0 = 0.48$. Rarefaction wave does not reach $r = 0$ before freeze-out. (b) $T_f/T_0 = \frac{1}{6}$. At τ_1, $T(r=0) = T_f$, freeze-out begins from $r = 0$.

$$G(\tau)=2\pi J^0 r_f \tau\left[v_r-\frac{\partial r_f}{\partial \tau}\right], \tag{5.17}$$

where J^0 and v_r are evaluated at T_f and $r_f(\tau)$, we then have

$$\langle p_T{}^n\rangle=(dN/dy)^{-1}\int_{\tau_0}^{\tau_f} p_T{}^n(T_f)G(\tau)d\tau+\langle p_T{}^n\rangle_{1,2}\ . \tag{5.18}$$

In the first case discussed in connection with (5.14), we have

$$\langle p_T{}^n\rangle_1=p_{T,\mathrm{th}}{}^n(dN_1/dy)(dN/dy)^{-1}\ , \tag{5.19}$$

where $p_{T,\mathrm{th}}$ is given by (5.7), while p_T in (5.18) is given by (5.9). In the second case we have, from (5.16),

$$\langle p_T{}^n\rangle_2=(dN/dy)^{-1}\int_{\tau_1}^{\tau_f} p_T{}^n(T_f)G'(\tau)d\tau\ , \tag{5.20}$$

where $G'(\tau)$ is $-G(\tau)$ as defined in (5.17) except that r_f and v_r are evaluated along the second branch, i.e., r_f' and v_r'.

The values for $\langle p_T\rangle$ and dN/dy can be computed, since have the numerical solution of the hydrodynamical problem. What we need as inputs are the values of τ_0, T_0, T_c, and T_f. In the absence of phase transition and transverse hydrodynamical expansion, the average transverse momentum is of thermal origin only and is independent of τ_0, T_0, T_c, and R. From either (5.7) or (5.9) we get

$$p_{T,\mathrm{th}}=2.627T_f\ . \tag{5.21}$$

Taking T_f to be 140 and 160 MeV as representative values, we have $p_{T,\mathrm{th}}=368$ and 420 MeV, respectively. In view of the canonical value of 350 MeV for the average p_T of pions produced in minimum-bias events in hadron-hadron collisions, we conclude that setting T_f at the pion mass is very reasonable. Nevertheless, we shall show below the results obtained using the two values of T_f, 140 and 160 MeV, since it is instructive to compare their differences.

In presenting the results of our calculation, we fix T_c at 200 MeV. For every pair of values of τ_0 and T_0, we can determine the corresponding values of $\langle p_T\rangle$ and dN/dy. Consequently, we can exhibit the dependence of $\langle p_T\rangle$ on dN/dy if we vary τ_0 and T_0 simultaneously in accordance to a constraint equation. Such a constraint is indeed available as a result of a study of the thermalization problem in nucleus-nucleus collisions. On the basis of the parton model it is found that[8]

$$T_0=180A^{1/6}\ \mathrm{MeV},\quad \tau_0=0.27A^{-1/6}\ \mathrm{fm}/c\ . \tag{5.22}$$

We therefore vary our values for T_0 and τ_0 along the curve

$$T_0\tau_0=49\ \mathrm{MeV\,fm}/c\cong 0.25\ . \tag{5.23}$$

Deviations from these constraints will be discussed later. The effective nuclear radius is related to A in the canonical way: $R=1.2A^{1/3}$ fm. Note that by varying along the constraint curve we are effectively varying the initial radius R before hydrodynamical expansion. This is a reasonable source of fluctuation even for fixed incident nuclear types, since the impact parameter fluctuates from collision to collision. Indeed, the large fluctuation in multiplicity distribution observed in hadron-hadron collisions at CERN ISR and SPS can be related to impact-parameter smearing.[14] Although at each fixed impact parameter, and therefore fixed R or effective number of participating nucleons, there can still be fluctuation in T_0, we shall regard that fluctuation to be minimal. This is one of the areas where our work differs from Ref. 6, where R is kept fixed for each nucleus in a reaction.

The results of our calculation are shown in Fig. 10 for $T_f=140$ and 160 MeV, and for the cases with and without phase transition. We see in Fig. 10 that collective transverse expansion increases $\langle p_T\rangle$ above $p_{T,\mathrm{th}}$, the increase being greater for the case with phase transition than without. The reason is that the phase transition slows down the cooling of the system so that higher transverse velocity can be developed before freeze-out occurs. Indeed, the lower the freeze-out temperature T_f, the greater is the net gain in transverse momentum due to collective expansion. Note that the difference between the two solid curves in Fig. 10 (corresponding to two values of T_f, both with phase transition) is smaller than the difference between the two values of $p_{T,\mathrm{th}}$ (for which there is no transverse expansion at all). The implication is very important for our general conclusion to be drawn later: When the collective motion is taken into account, the case with lower T_f allows the system to develop more transverse velocity before freeze-out so that the lesser thermal contribution to $\langle p_T\rangle$ is compensated by the greater collective hydrodynamical contribution.

It is also evident in Fig. 10 that after the initial rise of $\langle p_T\rangle$ with dN/dy, further increase is gradual and at a diminishing rate. This characteristic is independent of whether there is a phase transition. To see which part of

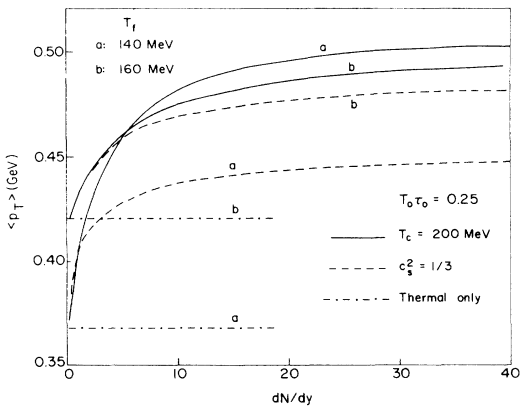

FIG. 10. Average transverse momentum vs rapidity density for two values of T_f: (a) 140 MeV; (b) 160 MeV. Solid lines are for phase transition at $T_c=200$ MeV, dashed lines for no phase transition, and dashed-dotted lines for no hydrodynamical expansion, i.e., $\langle p_T\rangle=p_{T,\mathrm{th}}$. The curves are obtained using $R=1.2A^{1/3}$ fm, $T_0=180A^{1/6}$ MeV, and $T_0\tau_0=0.25$. Variations along the curves are effected by varying A, or equivalently the impact parameter.

the curve corresponds to T_0 being in the neighborhood of T_c, we have calculated dN/dy as a function of T_0, but plotted it the other way around in Fig. 11. Near 200 MeV, which is the value of T_c used in all our calculations, the value of dN/dy for the case with phase transition increases precipitously by about a factor of 10 compared to the case without phase transition, just as one would expect by counting the increase in the degree of freedom, a property of the system that has been introduced through the ratio A/B in (3.6). (This is the "plateau" region referred to in Refs. 4 and 5, but here it is T_0, not $\langle p_T \rangle$.) Over the corresponding range of dN/dy, we see, however, in Fig. 10 that $\langle p_T \rangle$ rises most steeply. This results disagrees with the plateau behavior of $\langle p_T \rangle$ discussed in Refs. 4 and 5. The physical mechanism responsible for our result is that, as T_0 is increased over the T_c region in the case with phase transition, the time duration taken to reach freeze-out varies over a wide range; consequently, the transverse expansion permitted during that period also varies widely, leading to a sharp rise in $\langle p_T \rangle$. Further increase in T_0 does not lead to proportionally higher values of $\langle p_T \rangle$, because the plasma cools off rapidly from T_0 to T_c. As noted in the preceding paragraph, the value of $\langle p_T \rangle$ reflects more the hydrodynamical history of the expanding system than the thermodynamical state at either $T_0(\tau_0)$ or $T_f(\tau_f)$.

To see how sensitive our results are to the constraints on T_0 and τ_0 stated in (5.22) and (5.23), let it first be emphasized that those constraints are derived in Ref. 8 within the framework of a scaling parton model. If the initial parton density F_0 per nucleon in the central rapidity region increases with energy, as it must, since the observed plateau height of produce particles is nonscaling, then the coefficient of $A^{1/6}$ of T_0 in (5.22) would also increase as $F_0^{1/2}$, in accordance to Eq. (22) in Ref. 8. Moreover, the constraint expressed in (5.23) represents only a lower bound on τ_0, as discussed in Ref. 8; the actual value of τ_0 may be significantly higher than that expressed in (5.22) when the interactions among quarks and gluons during the thermalization process are fully taken into account. For our purpose here, let us relax (5.22) by introducing the parametrization

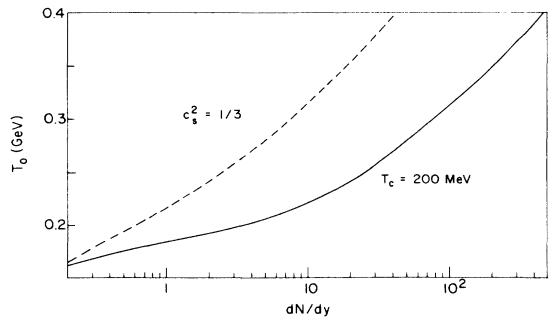

FIG. 11. Initial temperature vs rapidity density for the two cases with (solid) and without (dashed) phase transition. Other parameters are as in Fig. 10.

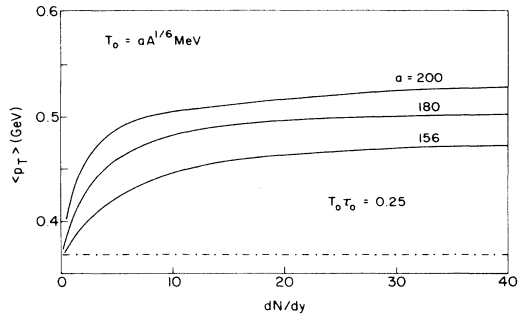

FIG. 12. Average transverse momentum vs rapidity density for $T_f=140$ MeV, $T_0\tau_0=0.25$, and three values of a in $T_0=aA^{1/6}$ MeV.

$$T_0=aA^{1/6}\ \text{MeV},\quad \tau_0=\frac{c}{a}A^{-1/6}\ . \tag{5.24}$$

We allow a to have the values 156, 180, and 200 MeV for $c=0.25$ and 0.5. The resultant curves for $\langle p_T \rangle$ are shown in Figs. 12 and 13 for the case with phase transition only and for $T_f=140$ MeV. We see that on the whole $\langle p_T \rangle$ increases with the values of a and c, but there is no change at all in the characteristics of the dependence of $\langle p_T \rangle$ on dN/dy. Thus the qualitative aspect of our result is independent of the details of the parametrization used. In summary, above $p_{T,\text{th}}$, $\langle p_T \rangle$ depends mainly on the collective expansion of the system, which in turn depends on whether T_0 is high enough to permit adequate time during phase transition for it to develop.

The result in Ref. 6 indicates a steeper increase in $\langle p_T \rangle$ versus dN/dy than ours after the initial rise. We have traced the origin of the discrepancy to the differences in how fluctuations are introduced. We allow variation in impact parameter so the effective nuclear size fluctuates, while in Ref. 6 R is fixed but T_0 is allowed to fluctuate. By allowing R to increase as T_0^2, we have found that above T_c the resultant increase in dN/dy is far more than that in $\langle p_T \rangle$. That is why the portion of the curves in Fig. 10 above the initial rise has diminishing slope. We have been able to reproduce largely the result in Ref. 6 when we fix R, as is done there.

We have also calculated $dN/dy\,dp_T{}^2$ at $y=0$. Since

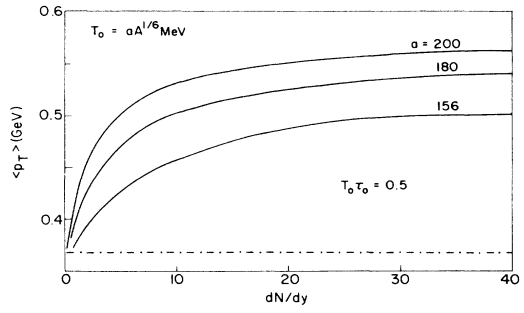

FIG. 13. Same as in Fig. 12, except that $T_0\tau_0=0.5$.

$$\frac{dN}{dy\,dp_T^2}=\frac{dN/dy\,d\tau}{dp_T^2/d\tau}\ , \tag{5.25}$$

the numerator can be determined from (5.13) by differentiation, and the denominator from (5.9) where $T=T_f$ and α is given by (2.7) evaluated at τ_f. An alternative but equivalent method is first to calculate, from (5.1),

$$\frac{d\mathcal{N}}{dk_T^2}=(g_\pi/16\pi^3\cosh\alpha)\int dk_L d\phi[\exp(k\cdot u/T)-1]^{-1} \tag{5.26}$$

and then to perform the hydrodynamical average

$$\frac{dN}{dy\,dp_T^2}=\int_{\tau_0}^{\tau_f}\left[\frac{d\mathcal{N}}{dk_T^2}\right]_{k_T^2=p_T^2}\frac{G(\tau)}{\mathcal{N}}d\tau+\frac{dN_{1,2}}{dy\,dp_T^2}\ , \tag{5.27}$$

where

$$\frac{dN_1}{dy\,dp_T^2}=\pi R_f^2\tau_f\frac{d\mathcal{N}}{dk_T^2}\bigg|_{k_T^2=p_T^2}\ , \tag{5.28}$$

$$\frac{dN_2}{dy\,dp_T^2}=\int_{\tau_1}^{\tau_f}\left[\frac{d\mathcal{N}}{dk_T^2}\right]_{k_T^2=p_T^2}\frac{G'(\tau)}{\mathcal{N}}d\tau\ . \tag{5.29}$$

The results of our calculation for the parameters in (5.22) are shown in Fig. 14, for two representative values of dN/dy. The p_T distributions will be useful not only in comparison with data, when available, but also in determining higher moments $\langle p_T^n\rangle$, as we shall do in a sequel to this paper.[15]

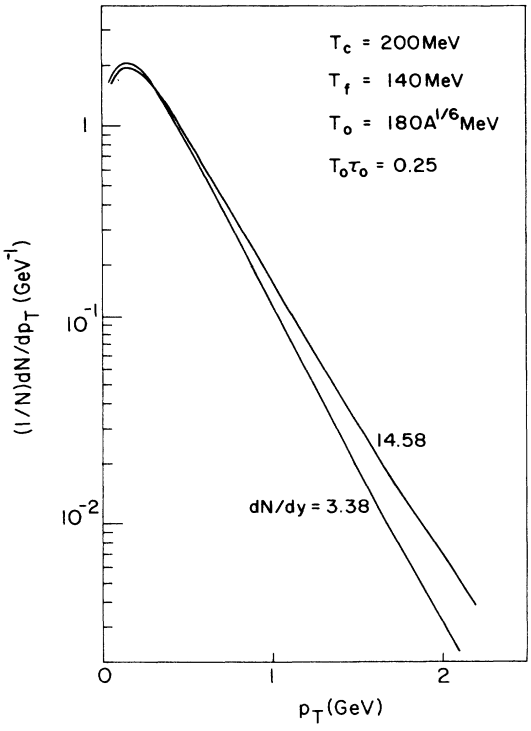

FIG. 14. Transverse-momentum distribution for the case with phase transition.

VI. CONCLUSION

We have made a quantitative study of the transverse momenta of hadrons produced in high-energy nucleus-nucleus collisions. Taking into account the statistical properties of the hadronic system in local thermodynamical equilibrium, we first obtain p_T as a function of T and v_r. The hydrodynamical expansion of the system including phase transition is then carefully considered in order to determine the time when the surface of the system reaches freeze-out temperature. It is the pions emitted at that time (at $T_f\cong m_\pi$) that are counted in the contribution to the p_T distribution. The resultant $\langle p_T\rangle$ is shown to increase rapidly at first with dN/dy, but then only gradually without any dramatic rise at high dN/dy. This result disagrees with the suggestion that $\langle p_T\rangle$ develops a plateau first, as dN/dy is increased, and then rises sharply at higher dN/dy.[4,5] It is on this difference that we now make some comments in conclusion.

It has been suggested that since $\langle p_T\rangle$ is an observable reflection of the temperature of the thermal system, a plateau in $\langle p_T\rangle$ as a function of dN/dy would be a consequence of a phase transition at which T remains approximately constant as the energy density undergoes a steplike increase due to deconfinement. Above T_c both $\langle p_T\rangle$ and dN/dy would increase, as the temperature and entropy would, if the nuclear collision can put the system in a hot plasma state with increasingly higher energy density.

In our view a plasma state with $T>T_c$ consists of quarks and gluons whose transverse momenta cannot be translated directly to the hadron p_T. The hadronization process, whether by fragmentation or recombination, undoubtedly will affect the p_T distribution, as is familiar in the parton-model description of the p_L distribution in soft hadronic production at low p_T.[16] Fragmentation of quarks and gluons leaving a plasms surface is a rather nontrivial problem, and is one that will be treated in some detail elsewhere.[15] Recombination is essentially what takes place during phase transition as the plasma condenses into a hadron gas, which continues to expand longitudinally as well as transversely, so that the detected hadrons do not stop interacting with other hadrons (and thereby changing their p_T values) until T drops from the transition temperature T_c to the freeze-out temperature T_f. Thus in this picture $\langle p_T\rangle$ cannot be related directly to the initial plasma temperature T_0 or any other value of T above T_f without accounting for the effects of collective expansion, and of hadronization at T_c and freeze-out at T_f. An approach treating the thermodynamical and hydrodynamical components of $\langle p_T\rangle$ as being additive is clearly not justified, since our calculation has shown that the relationship between $\langle p_T\rangle$ and dN/dy is a result of the intricate interdependence of T, v_r, r_f, and τ. Instead of a plateau followed by a precipitous rise, $\langle p_T\rangle$ rises sharply over the phase transition region due to the collective expansion, and then it increases only gently at a diminishing rate as dN/dy is increased. This result is a consequence of not holding the initial radius fixed, but allowing it to vary due to impact-parameter fluctuation. We believe that the significant increase in $\langle p_T\rangle$ observed both in $p\bar{p}$ collisions at the CERN SPS (Refs. 1 and 2) and

in cosmic-ray experiments (Ref. 3) are related to the production of minijets.[17]

In Fig. 10 we do see that the occurrence of phase transition increases the value of $\langle p_T \rangle$ over the entire range of dN/dy, when compared to the case without phase transition. However, to identify that increase above the background would be phenomenologically very difficult, especially in view of the expected competing mechanism arising from minijets. The use of $\langle p_T \rangle$ as a signature for quark-gluon plasma is therefore far more complex than first realized.

ACKNOWLEDGMENTS

We are grateful to G. Baym, J. Kapusta, C. S. Lam, and L. McLerran for helpful discussions, communications, and assistance. This work was supported in part by the U.S. Department of Energy under Grant No. DEFG0685ER40224-A001.

[1]G. Arnison *et al.*, Phys. Lett. **118B**, 167 (1982).
[2]A. Breakstone *et al.*, Phys. Lett. **115B**, 64 (1982).
[3]T. H. Burnett *et al.*, Phys. Rev. Lett. **50**, 2062 (1983).
[4]L. Van Hove, Phys. Lett. **118B**, 138 (1982).
[5]J. Kapusta, S. Pratt, L. McLerran, and H. von Gersdorff, Phys. Lett. **163B**, 253 (1985).
[6]H. von Gersdorff, L. McLerran, M. Kataja, and P. V. Ruuskanen, Phys. Rev. D **34**, 794 (1986); M. Kataja, P. V. Ruuskanen, L. D. McLerran, and H. von Gersdorff, *ibid.* **34**, 2755 (1986).
[7]T. Celik, J. Engels, and H. Satz, Nucl. Phys. **B256**, 670 (1985).
[8]R. C. Hwa and K. Kajantie, Phys. Rev. Lett. **56**, 696 (1986).
[9]J.-P. Blaizot and J.-Y. Ollitrault, Nucl. Phys. **A458**, 745 (1986).
[10]J. D. Bjorken, Phys. Rev. D **27**, 140 (1983).
[11]G. Baym, B. L. Friman, J. P. Blaizot, M. Soyeur, and W. Czyz, Nucl. Phys. Lett. **A407**, 541 (1983).
[12]K. Redlich and H. Satz, Phys. Rev. D **33**, 3747 (1986).
[13]We are grateful to Professor Gordon Baym for providing assistance to us in the numerical integration.
[14]See, for example, S. Barshay, Phys. Lett. **116B**, 193 (1982); W. R. Chen and R. C. Hwa, Phys. Rev. D (to be published).
[15]See articles by A. Capella, R. C. Hwa, and U. P. Sukhatme, in *Partons in Soft-Hadronic Processes,* edited by R. T. Van de Walle (World Scientific, Singapore, 1981).
[16]T. Sjostrand, in *Proceedings of Physics Simulations at High Energy,* Madison, 1986, edited by V. Barger, T. Gottschalk, and F. Halzen (World Scientific, Singapore, 1987).
[17]R. C. Hwa and X.-N. Wang (unpublished).